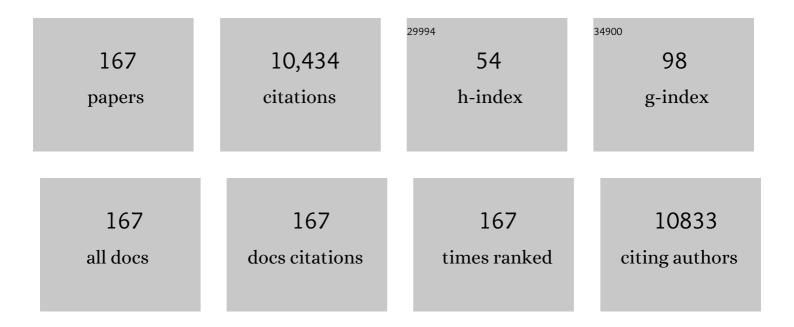
Whitney B Pope

List of Publications by Year in descending order

Source: https://exaly.com/author-pdf/9480834/publications.pdf Version: 2024-02-01



#	Article	IF	CITATIONS
1	Amineâ€weighted chemical exchange saturation transfer magnetic resonance imaging in brain tumors. NMR in Biomedicine, 2023, 36, .	1.6	7
2	Characterization of cognitive function in survivors of diffuse gliomas using resting-state functional MRI (rs-fMRI). Brain Imaging and Behavior, 2022, 16, 239-251.	1.1	5
3	Imaging Advances for Central Nervous System Tumors. Hematology/Oncology Clinics of North America, 2022, 36, 43-61.	0.9	4
4	Diffusion MRI is an early biomarker of overall survival benefit in IDH wild-type recurrent glioblastoma treated with immune checkpoint inhibitors. Neuro-Oncology, 2022, 24, 1020-1028.	0.6	12
5	Radiomics for precision medicine in glioblastoma. Journal of Neuro-Oncology, 2022, 156, 217-231.	1.4	22
6	Visualization of tumor heterogeneity and prediction of isocitrate dehydrogenase mutation status for human gliomas using multiparametric physiologic and metabolic MRI. Scientific Reports, 2022, 12, 1078.	1.6	5
7	Paradoxical Association Between Relative Cerebral Blood Volume Dynamics Following Chemoradiation and Increased Progression-Free Survival in Newly Diagnosed IDH Wild-Type MGMT Promoter Methylated Glioblastoma With Measurable Disease. Frontiers in Oncology, 2022, 12, 849993.	1.3	1
8	Diagnostic and Prognostic Value of pH- and Oxygen-Sensitive Magnetic Resonance Imaging in Glioma: A Retrospective Study. Cancers, 2022, 14, 2520.	1.7	2
9	Characterization of Cognitive Function in Survivors of Diffuse Gliomas Using Morphometric Correlation Networks. Tomography, 2022, 8, 1437-1452.	0.8	0
10	Voxelwise and Patientwise Correlation of ¹⁸ F-FDOPA PET, Relative Cerebral Blood Volume, and Apparent Diffusion Coefficient in Treatment-Naà ve Diffuse Cliomas with Different Molecular Subtypes. Journal of Nuclear Medicine, 2021, 62, 319-325.	2.8	13
11	Relative oxygen extraction fraction (rOEF) MR imaging reveals higher hypoxia in human epidermal growth factor receptor (EGFR) amplified compared with non-amplified gliomas. Neuroradiology, 2021, 63, 857-868.	1.1	7
12	Differentiating IDH status in human gliomas using machine learning and multiparametric MR/PET. Cancer Imaging, 2021, 21, 27.	1.2	13
13	Using non-invasive neuroimaging to enhance the care, well-being and experimental outcomes of laboratory non-human primates (monkeys). NeuroImage, 2021, 228, 117667.	2.1	13
14	Preferential tumor localization in relation to 18F-FDOPA uptake for lowerâ€grade gliomas. Journal of Neuro-Oncology, 2021, 152, 573-582.	1.4	2
15	Worse prognosis for IDH wild-type diffuse gliomas with larger residual biological tumor burden. Annals of Nuclear Medicine, 2021, 35, 1022-1029.	1.2	5
16	NIMG-74. RESPONSE ASSESSMENT AFTER DOSE-ESCALATED RADIOTHERAPY: IMAGING PROTOCOL OF A MULTICENTER PHASE III TRIAL ON INTRAOPERATIVE RADIOTHERAPY IN NEWLY DIAGNOSED GLIOBLASTOMA (INTRAGO-II;ARO2016-1;AG-NRO-03). Neuro-Oncology, 2021, 23, vi146-vi146.	0.6	0
17	NIMG-41. PH-WEIGHTED MOLECULAR MRI AS AN EARLY BIOMARKER OF METABOLIC RESPONSE TO IDH INHIBITION IN IDH MUTANT GLIOMAS. Neuro-Oncology, 2021, 23, vi138-vi138.	0.6	0
18	"Aerobic glycolytic imaging―of human gliomas using combined pH-, oxygen-, and perfusion-weighted magnetic resonance imaging. Neurolmage: Clinical, 2021, 32, 102882.	1.4	8

#	Article	IF	CITATIONS
19	NIMG-36. VISUALIZATION OF TUMOR HETEROGENEITY AND PREDICTION OF ISOCITRATE DEHYDROGENASE MUTATION STATUS FOR HUMAN GLIOMAS BY USING MULTIPARAMETRIC PHYSIOLOGIC AND METABOLIC MRI. Neuro-Oncology, 2021, 23, vi136-vi137.	0.6	0
20	NIMG-44. PROGNOSTIC VALUE OF PH- AND OXYGEN-SENSITIVE MRI IN GLIOMA PATIENTS. Neuro-Oncology, 2021, 23, vi138-vi139.	0.6	0
21	Longitudinal MRI findings in patients with newly diagnosed glioblastoma after intraoperative radiotherapy. Journal of Neuroradiology, 2020, 47, 166-173.	0.6	6
22	Imaging challenges of immunotherapy and targeted therapy in patients with brain metastases: response, progression, and pseudoprogression. Neuro-Oncology, 2020, 22, 17-30.	0.6	94
23	Human IDH mutant 1p/19q co-deleted gliomas have low tumor acidity as evidenced by molecular MRI and PET: a retrospective study. Scientific Reports, 2020, 10, 11922.	1.6	23
24	Multiparametric MR-PET measurements in hypermetabolic regions reflect differences in molecular status and tumor grade in treatment-naÃ ⁻ ve diffuse gliomas. Journal of Neuro-Oncology, 2020, 149, 337-346.	1.4	5
25	Decorin expression is associated with predictive diffusion MR phenotypes of anti-VEGF efficacy in glioblastoma. Scientific Reports, 2020, 10, 14819.	1.6	13
26	Diffusion Magnetic Resonance Imaging Phenotypes Predict Overall Survival Benefit From Bevacizumab or Surgery in Recurrent Glioblastoma With Large Tumor Burden. Neurosurgery, 2020, 87, 931-938.	0.6	14
27	The MRI Features and Prognosis of Cliomas Associated With IDH1 Mutation: A Single Center Study in Southwest China. Frontiers in Oncology, 2020, 10, 852.	1.3	9
28	Diffusion MRI changes in the anterior subventricular zone following chemoradiation in glioblastoma with posterior ventricular involvement. Journal of Neuro-Oncology, 2020, 147, 643-652.	1.4	5
29	Rate of change in maximum 18F-FDOPA PET uptake and non-enhancing tumor volume predict malignant transformation and overall survival in low-grade gliomas. Journal of Neuro-Oncology, 2020, 147, 135-145.	1.4	12
30	Glioblastoma Utilizes Fatty Acids and Ketone Bodies for Growth Allowing Progression during Ketogenic Diet Therapy. IScience, 2020, 23, 101453.	1.9	47
31	Association between Tumor Acidity and Hypervascularity in Human Gliomas Using pH-Weighted Amine Chemical Exchange Saturation Transfer Echo-Planar Imaging and Dynamic Susceptibility Contrast Perfusion MRI at 3T. American Journal of Neuroradiology, 2019, 40, 979-986.	1.2	24
32	Metabolic characterization of human IDH mutant and wild type gliomas using simultaneous pH- and oxygen-sensitive molecular MRI. Neuro-Oncology, 2019, 21, 1184-1196.	0.6	28
33	Validation of vessel size imaging (VSI) in high-grade human gliomas using magnetic resonance imaging, image-guided biopsies, and quantitative immunohistochemistry. Scientific Reports, 2019, 9, 2846.	1.6	32
34	Recent developments and future directions in adult lower-grade gliomas: Society for Neuro-Oncology (SNO) and European Association of Neuro-Oncology (EANO) consensus. Neuro-Oncology, 2019, 21, 837-853.	0.6	66
35	pH-weighted amine chemical exchange saturation transfer echoplanar imaging (CEST-EPI) as a potential early biomarker for bevacizumab failure in recurrent glioblastoma. Journal of Neuro-Oncology, 2019, 142, 587-595.	1.4	28
36	PET imaging in patients with brain metastasis—report of the RANO/PET group. Neuro-Oncology, 2019, 21, 585-595.	0.6	139

#	Article	IF	CITATIONS
37	18F-FDOPA PET and MRI characteristics correlate with degree of malignancy and predict survival in treatment-naÃ ⁻ ve gliomas: a cross-sectional study. Journal of Neuro-Oncology, 2018, 139, 399-409.	1.4	32
38	Post-chemoradiation volumetric response predicts survival in newly diagnosed glioblastoma treated with radiation, temozolomide, and bevacizumab or placebo. Neuro-Oncology, 2018, 20, 1525-1535.	0.6	15
39	Validation of postoperative residual contrast-enhancing tumor volume as an independent prognostic factor for overall survival in newly diagnosed glioblastoma. Neuro-Oncology, 2018, 20, 1240-1250.	0.6	64
40	Simultaneous p <scp>H</scp> â€sensitive and oxygenâ€sensitive <scp>MRI</scp> of human gliomas at 3 <scp>T</scp> using multiâ€echo amine proton chemical exchange saturation transfer spinâ€endâ€gradient echo echoâ€planar imaging (<scp>CESTâ€SAGEâ€EPI</scp>). Magnetic Resonance in Medicine, 2018, 80, 1962-1978.	1.9	38
41	Improved Spatiotemporal Resolution of Dynamic Susceptibility Contrast Perfusion MRI in Brain Tumors Using Simultaneous Multi-Slice Echo-Planar Imaging. American Journal of Neuroradiology, 2018, 39, 43-45.	1.2	15
42	Phase 2 Study of Bortezomib Combined With Temozolomide and Regional Radiation Therapy for Upfront Treatment of Patients With Newly Diagnosed Glioblastoma Multiforme: Safety and Efficacy Assessment. International Journal of Radiation Oncology Biology Physics, 2018, 100, 1195-1203.	0.4	45
43	Conventional and advanced magnetic resonance imaging in patients with high-grade glioma. Quarterly Journal of Nuclear Medicine and Molecular Imaging, 2018, 62, 239-253.	0.4	63
44	Mono-exponential, diffusion kurtosis and stretched exponential diffusion MR imaging response to chemoradiation in newly diagnosed glioblastoma. Journal of Neuro-Oncology, 2018, 139, 651-659.	1.4	25
45	Gadolinium deposition within the paediatric brain: no increased intrinsic T1-weighted signal intensity within the dentate nucleus following the administration of a minimum of four doses of the macrocyclic agent gadobutrol. European Radiology, 2018, 28, 4882-4889.	2.3	12
46	Gadolinium Deposition within the Pediatric Brain: No Increased Intrinsic T1-Weighted Signal Intensity within the Dentate Nucleus following the Administration of a Minimum of 4 Doses of the Macrocyclic Agent Gadoteridol. American Journal of Neuroradiology, 2018, 39, 1604-1608.	1.2	16
47	Brain metastases: neuroimaging. Handbook of Clinical Neurology / Edited By P J Vinken and G W Bruyn, 2018, 149, 89-112.	1.0	123
48	Improving B0 Correction for pH-Weighted Amine Proton Chemical Exchange Saturation Transfer (CEST) Imaging by Use of k-Means Clustering and Lorentzian Estimation. Tomography, 2018, 4, 123-137.	0.8	16
49	Longitudinal DSC-MRI for Distinguishing Tumor Recurrence From Pseudoprogression in Patients With a High-grade Glioma. American Journal of Clinical Oncology: Cancer Clinical Trials, 2017, 40, 228-234.	0.6	77
50	The use of amino acid PET and conventional MRI for monitoring of brain tumor therapy. NeuroImage: Clinical, 2017, 13, 386-394.	1.4	101
51	Perfusion and diffusion MRI signatures in histologic and genetic subtypes of WHO grade Il–III diffuse gliomas. Journal of Neuro-Oncology, 2017, 134, 177-188.	1.4	118
52	Pseudoprogression, radionecrosis, inflammation or true tumor progression? challenges associated with glioblastoma response assessment in an evolving therapeutic landscape. Journal of Neuro-Oncology, 2017, 134, 495-504.	1.4	160
53	Evaluation of Magnetonanoparticles Conjugated with New Angiogenesis Peptides in Intracranial Glioma Tumors by MRI. Applied Biochemistry and Biotechnology, 2017, 183, 265-279.	1.4	13
54	Application of arterial spin labeling perfusion MRI to differentiate benign from malignant intracranial meningiomas. European Journal of Radiology, 2017, 97, 31-36.	1.2	42

#	Article	IF	CITATIONS
55	Diffusion MRI Phenotypes Predict Overall Survival Benefit from Anti-VEGF Monotherapy in Recurrent Glioblastoma: Converging Evidence from Phase II Trials. Clinical Cancer Research, 2017, 23, 5745-5756.	3.2	53
56	Multiple calcifying pseudoneoplasms of the neuraxis (MCAPNON): Distinct entity, CAPNON variant, or old neurocysticercosis?. Neuropathology, 2017, 37, 233-240.	0.7	17
57	Baseline pretreatment contrast enhancing tumor volume including central necrosis is a prognostic factor in recurrent glioblastoma: evidence from single and multicenter trials. Neuro-Oncology, 2017, 19, 89-98.	0.6	68
58	Molecular Imaging of Diffuse Low Grade Glioma. , 2017, , 173-195.		0
59	Improved Leakage Correction for Single-Echo Dynamic Susceptibility Contrast Perfusion MRI Estimates of Relative Cerebral Blood Volume in High-Grade Gliomas by Accounting for Bidirectional Contrast Agent Exchange. American Journal of Neuroradiology, 2016, 37, 1440-1446.	1.2	39
60	Response Assessment in Neuro-Oncology working group and European Association for Neuro-Oncology recommendations for the clinical use of PET imaging in gliomas. Neuro-Oncology, 2016, 18, 1199-1208.	0.6	566
61	Two cases of rheumatoid meningitis. Neuropathology, 2016, 36, 93-102.	0.7	43
62	Dynamic Susceptibility Contrast MR Imaging in Glioma. Magnetic Resonance Imaging Clinics of North America, 2016, 24, 649-670.	0.6	43
63	Simulation, phantom validation, and clinical evaluation of fast pHâ€weighted molecular imaging using amine chemical exchange saturation transfer echo planar imaging (CESTâ€EPI) in glioma at 3 T. NMR in Biomedicine, 2016, 29, 1563-1576.	1.6	51
64	Contrastâ€enhancing tumor growth dynamics of preoperative, treatmentâ€naive human glioblastoma. Cancer, 2016, 122, 1718-1727.	2.0	47
65	Blood-Labyrinth Barrier Permeability in Menière Disease and Idiopathic Sudden Sensorineural Hearing Loss: Findings on Delayed Postcontrast 3D-FLAIR MRI. American Journal of Neuroradiology, 2016, 37, 1903-1908.	1.2	67
66	Neuroimaging. Handbook of Clinical Neurology / Edited By P J Vinken and G W Bruyn, 2016, 134, 27-50.	1.0	6
67	Bidirectional Contrast agent leakage correction of dynamic susceptibility contrast (DSC)â€MRI improves cerebral blood volume estimation and survival prediction in recurrent glioblastoma treated with bevacizumab. Journal of Magnetic Resonance Imaging, 2016, 44, 1229-1237.	1.9	27
68	The Impact of T2/FLAIR Evaluation per RANO Criteria on Response Assessment of Recurrent Glioblastoma Patients Treated with Bevacizumab. Clinical Cancer Research, 2016, 22, 575-581.	3.2	62
69	Physiologic MRI for assessment of response to therapy and prognosis in glioblastoma. Neuro-Oncology, 2016, 18, 467-478.	0.6	67
70	Between-Scanner and Between-Visit Variation in Normal White Matter Apparent Diffusion Coefficient Values in the Setting of a Multi-Center Clinical Trial. Clinical Neuroradiology, 2016, 26, 423-430.	1.0	18
71	Modeling the efficacy of the extent of surgical resection in the setting of radiation therapy for glioblastoma. Cancer Science, 2016, 107, 1110-1116.	1.7	16
72	Association between lesion location and language function in adult glioma using voxel-based lesion-symptom mapping. NeuroImage: Clinical, 2015, 9, 617-624.	1.4	23

#	Article	IF	CITATIONS
73	NIMG-24HIGH SPATIOTEMPORAL DYNAMIC SUSCEPTIBILITY CONTRAST (DSC) PERFUSION MRI USING MULTIBAND ECHOPLANAR IMAGING (MB-EPI). Neuro-Oncology, 2015, 17, v158.4-v159.	0.6	70
74	Evidence for rCBV as an early response marker following bevacizumab treatment. Neuro-Oncology, 2015, 17, 1539-1540.	0.6	2
75	A novel bicompartmental mathematical model of glioblastoma multiforme. International Journal of Oncology, 2015, 46, 825-832.	1.4	5
76	Patient-specific characterization of the invasiveness and proliferation of low-grade gliomas using serial MR imaging and a mathematical model of tumor growth. Oncology Reports, 2015, 33, 2883-2888.	1.2	5
77	Nitroxoline induces apoptosis and slows glioma growth in vivo. Neuro-Oncology, 2015, 17, 53-62.	0.6	41
78	From the clinician's point of view - What is the status quo of positron emission tomography in patients with brain tumors?. Neuro-Oncology, 2015, 17, 1434-1444.	0.6	144
79	Predictive imaging marker of bevacizumab efficacy: perfusion MRI: TableÂ1 Neuro-Oncology, 2015, 17, 1046-1047.	0.6	11
80	MRI perfusion measurements calculated using advanced deconvolution techniques predict survival in recurrent glioblastoma treated with bevacizumab. Journal of Neuro-Oncology, 2015, 122, 497-505.	1.4	37
81	Relationship Between [18F]FDOPA PET Uptake, Apparent Diffusion Coefficient (ADC), and Proliferation Rate in Recurrent Malignant Gliomas. Molecular Imaging and Biology, 2015, 17, 434-442.	1.3	28
82	Quantification of Nonenhancing Tumor Burden in Gliomas Using Effective T2 Maps Derived from Dual-Echo Turbo Spin-Echo MRI. Clinical Cancer Research, 2015, 21, 4373-4383.	3.2	27
83	Immunotherapy response assessment in neuro-oncology: a report of the RANO working group. Lancet Oncology, The, 2015, 16, e534-e542.	5.1	582
84	pH-weighted molecular imaging of gliomas using amine chemical exchange saturation transfer MRI. Neuro-Oncology, 2015, 17, 1514-1524.	0.6	96
85	Consensus recommendations for a standardized Brain Tumor Imaging Protocol in clinical trials. Neuro-Oncology, 2015, 17, 1188-98.	0.6	346
86	Standardized Brain Tumor Imaging Protocol for Clinical Trials. American Journal of Neuroradiology, 2015, 36, E65-E66.	1.2	4
87	Radial expansion rates and tumor growth kinetics predict malignant transformation in contrast-enhancing low-grade diffuse astrocytoma. CNS Oncology, 2015, 4, 247-256.	1.2	16
88	Genomics of Brain Tumor Imaging. Neuroimaging Clinics of North America, 2015, 25, 105-119.	0.5	33
89	Diffusion MRI Characteristics after Concurrent Radiochemotherapy Predicts Progression-Free and Overall Survival in Newly Diagnosed Glioblastoma. Tomography, 2015, 1, 37-43.	0.8	12
90	Increased sensitivity to radiochemotherapy in IDH1 mutant glioblastoma as demonstrated by serial quantitative MR volumetry. Neuro-Oncology, 2014, 16, 414-420.	0.6	82

#	Article	IF	CITATIONS
91	Hypervascular tumor volume estimated by comparison to a large-scale cerebral blood volume radiographic atlas predicts survival in recurrent glioblastoma treated with bevacizumab. Cancer Imaging, 2014, 14, 31.	1.2	21
92	Report of the Jumpstarting Brain Tumor Drug Development Coalition and FDA clinical trials neuroimaging endpoint workshop (January 30, 2014, Bethesda MD). Neuro-Oncology, 2014, 16, vii36-vii47.	0.6	41
93	Emerging techniques and technologies in brain tumor imaging. Neuro-Oncology, 2014, 16, vii12-vii23.	0.6	41
94	BI-10 * pH-WEIGHTED MRI IN HUMAN GLIOMAS. Neuro-Oncology, 2014, 16, v25-v25.	0.6	0
95	Recurrent Glioblastoma Treated with Bevacizumab: Contrast-enhanced T1-weighted Subtraction Maps Improve Tumor Delineation and Aid Prediction of Survival in a Multicenter Clinical Trial. Radiology, 2014, 271, 200-210.	3.6	150
96	Treatment Response Evaluation Using 18F-FDOPA PET in Patients with Recurrent Malignant Glioma on Bevacizumab Therapy. Clinical Cancer Research, 2014, 20, 3550-3559.	3.2	115
97	Deferred use of bevacizumab for recurrent glioblastoma is not associated with diminished efficacy. Neuro-Oncology, 2014, 16, 815-822.	0.6	49
98	Regional and Voxelâ€Wise Comparisons of Blood Flow Measurements Between Dynamic Susceptibility Contrast Magnetic Resonance Imaging (DSCâ€MRI) and Arterial Spin Labeling (ASL) in Brain Tumors. Journal of Neuroimaging, 2014, 24, 23-30.	1.0	45
99	Altered functional connectivity of the default mode network in diffuse gliomas measured with pseudo-resting state fMRI. Journal of Neuro-Oncology, 2014, 116, 373-379.	1.4	95
100	C-terminally truncated form of αB-crystallin is associated with IDH1 R132H mutation in anaplastic astrocytoma. Journal of Neuro-Oncology, 2014, 117, 53-65.	1.4	9
101	Facing the Future of Brain Tumor Clinical Research. Clinical Cancer Research, 2014, 20, 5591-5600.	3.2	4
102	Nonlinear distortion correction of diffusion MR images improves quantitative DTI measurements in glioblastoma. Journal of Neuro-Oncology, 2014, 116, 551-558.	1.4	12
103	Short-interval estimation of proliferation rate using serial diffusion MRI predicts progression-free survival in newly diagnosed glioblastoma treated with radiochemotherapy. Journal of Neuro-Oncology, 2014, 116, 601-608.	1.4	6
104	Intraoperative mass spectrometry of tumor metabolites. Proceedings of the National Academy of Sciences of the United States of America, 2014, 111, 10906-10907.	3.3	3
105	Isolated Choroid Plexus Granulomas: Initial Presentation of Neurosarcoidosis?. Canadian Journal of Neurological Sciences, 2014, 41, 112-114.	0.3	0
106	Validation of rano criteria: Contribution of T2/FLAIR assessment in patients with recurrent glioblastoma treated with bevacizumab Journal of Clinical Oncology, 2014, 32, 2007-2007.	0.8	3
107	Pre- and post-contrast three-dimensional double inversion-recovery MRI in human glioblastoma. Journal of Neuro-Oncology, 2013, 112, 257-266.	1.4	13
108	Imaging biomarkers for antiangiogenic therapy in malignant gliomas. CNS Oncology, 2013, 2, 33-47.	1.2	17

#	Article	IF	CITATIONS
109	Ensemble segmentation for GBM brain tumors on MR images using confidenceâ€based averaging. Medical Physics, 2013, 40, 093502.	1.6	12
110	Primary central nervous system histiocytic sarcoma presenting as a postradiation sarcoma: case report and literature review. Human Pathology, 2013, 44, 1177-1183.	1.1	34
111	PET Parametric Response Mapping for Clinical Monitoring and Treatment Response Evaluation in Brain Tumors. PET Clinics, 2013, 8, 201-217.	1.5	8
112	Magnetic Resonance Imaging of Glioma in the Era of Antiangiogenic Therapy. PET Clinics, 2013, 8, 163-182.	1.5	4
113	Multi-delay multi-parametric arterial spin-labeled perfusion MRI in acute ischemic stroke — Comparison with dynamic susceptibility contrast enhanced perfusion imaging. NeuroImage: Clinical, 2013, 3, 1-7.	1.4	180
114	Functionalized Magnetonanoparticles in Visualization of Intracranial Tumors on MRI. Molecular Imaging and Biology, 2013, 15, 299-306.	1.3	4
115	Combined analysis of O6-methylguanine-DNA methyltransferase protein expression and promoter methylation provides optimized prognostication of glioblastoma outcome. Neuro-Oncology, 2013, 15, 370-381.	0.6	97
116	Brainstem Gliomas. , 2013, 18, 237-242.		0
117	Identifying the mesenchymal molecular subtype of glioblastoma using quantitative volumetric analysis of anatomic magnetic resonance images. Neuro-Oncology, 2013, 15, 626-634.	0.6	91
118	Reply:. American Journal of Neuroradiology, 2013, 34, E12-E12.	1.2	0
119	Quantitative probabilistic functional diffusion mapping in newly diagnosed glioblastoma treated with radiochemotherapy. Neuro-Oncology, 2013, 15, 382-390.	0.6	38
120	Functional diffusion maps (fDMs) evaluated before and after radiochemotherapy predict progression-free and overall survival in newly diagnosed glioblastoma. Neuro-Oncology, 2012, 14, 333-343.	0.6	74
121	3′-Deoxy-3′- ¹⁸ F-Fluorothymidine PET and MRI for Early Survival Predictions in Patients with Recurrent Malignant Glioma Treated with Bevacizumab. Journal of Nuclear Medicine, 2012, 53, 29-36.	2.8	122
122	The Value of Arterial Spin-Labeled Perfusion Imaging in Acute Ischemic Stroke. Stroke, 2012, 43, 1018-1024.	1.0	151
123	18F-FDOPA and 18F-FLT positron emission tomography parametric response maps predict response in recurrent malignant gliomas treated with bevacizumab. Neuro-Oncology, 2012, 14, 1079-1089.	0.6	99
124	Detection of 2-hydroxyglutaric acid in vivo by proton magnetic resonance spectroscopy in U87 glioma cells overexpressing isocitrate dehydrogenase-1 mutation. Neuro-Oncology, 2012, 14, 1465-1472.	0.6	35
125	Anatomic localization of O6-methylguanine DNA methyltransferase (MGMT) promoter methylated and unmethylated tumors: A radiographic study in 358 de novo human glioblastomas. NeuroImage, 2012, 59, 908-916.	2.1	128
126	Current Concepts in Brain Tumor Imaging. American Society of Clinical Oncology Educational Book / ASCO American Society of Clinical Oncology Meeting, 2012, , 119-124.	1.8	3

#	Article	IF	CITATIONS
127	Comparison between intensity normalization techniques for dynamic susceptibility contrast (DSC)â€MRI estimates of cerebral blood volume (CBV) in human gliomas. Journal of Magnetic Resonance Imaging, 2012, 35, 1472-1477.	1.9	68
128	Apparent diffusion coefficient histogram analysis stratifies progression-free and overall survival in patients with recurrent GBM treated with bevacizumab: a multi-center study. Journal of Neuro-Oncology, 2012, 108, 491-498.	1.4	149
129	Nonlinear registration of diffusionâ€weighted images improves clinical sensitivity of functional diffusion maps in recurrent glioblastoma treated with bevacizumab. Magnetic Resonance in Medicine, 2012, 67, 237-245.	1.9	36
130	Quantification of edema reduction using differential quantitative T2 (DQT2) relaxometry mapping in recurrent glioblastoma treated with bevacizumab. Journal of Neuro-Oncology, 2012, 106, 111-119.	1.4	67
131	Non-invasive detection of 2-hydroxyglutarate and other metabolites in IDH1 mutant glioma patients using magnetic resonance spectroscopy. Journal of Neuro-Oncology, 2012, 107, 197-205.	1.4	280
132	High Order Diffusion Tensor Imaging in Human Glioblastoma. Academic Radiology, 2011, 18, 947-954.	1.3	10
133	Sampling-based ensemble segmentation against inter-operator variability. Proceedings of SPIE, 2011, , .	0.8	2
134	Cell invasion, motility, and proliferation level estimate (CIMPLE) maps derived from serial diffusion MR images in recurrent glioblastoma treated with bevacizumab. Journal of Neuro-Oncology, 2011, 105, 91-101.	1.4	33
135	Advances in MRI Assessment of Gliomas and Response to Anti-VEGF Therapy. Current Neurology and Neuroscience Reports, 2011, 11, 336-344.	2.0	98
136	Evidence for Sequenced Molecular Evolution of <i>IDH1</i> Mutant Glioblastoma From a Distinct Cell of Origin. Journal of Clinical Oncology, 2011, 29, 4482-4490.	0.8	420
137	Quantitative volumetric analysis of conventional MRI response in recurrent glioblastoma treated with bevacizumab. Neuro-Oncology, 2011, 13, 401-409.	0.6	95
138	Graded functional diffusion map-defined characteristics of apparent diffusion coefficients predict overall survival in recurrent glioblastoma treated with bevacizumab. Neuro-Oncology, 2011, 13, 1151-1161.	0.6	69
139	Confidence-based ensemble for GBM brain tumor segmentation. , 2011, , .		1
140	Phase II Study of Bevacizumab Plus Temozolomide During and After Radiation Therapy for Patients With Newly Diagnosed Glioblastoma Multiforme. Journal of Clinical Oncology, 2011, 29, 142-148.	0.8	418
141	Insensitivity of visual assessment of hippocampal atrophy in familial Alzheimer's disease. Journal of Neurology, 2010, 257, 839-842.	1.8	17
142	Stem cell associated gene expression in glioblastoma multiforme: relationship to survival and the subventricular zone. Journal of Neuro-Oncology, 2010, 96, 359-367.	1.4	86
143	Update and developments in the treatment of glioblastoma multiforme – focus on bevacizumab. Pharmacogenomics and Personalized Medicine, 2010, 3, 79.	0.4	4
144	CADrx for GBM Brain Tumors: Predicting Treatment Response from Changes in Diffusion-Weighted MRI. Algorithms, 2009, 2, 1350-1367.	1.2	8

#	Article	IF	CITATIONS
145	Engagement of Fusiform Cortex and Disengagement of Lateral Occipital Cortex in the Acquisition of Radiological Expertise. Cerebral Cortex, 2009, 19, 2746-2754.	1.6	94
146	Histogram-based classification with Gaussian mixture modeling for GBM tumor treatment response using ADC map. , 2009, , .		4
147	Recurrent Clioblastoma Multiforme: ADC Histogram Analysis Predicts Response to Bevacizumab Treatment. Radiology, 2009, 252, 182-189.	3.6	317
148	18F-FDOPA PET/MRI fusion in patients with primary/recurrent gliomas: Initial experience. European Journal of Radiology, 2009, 71, 242-248.	1.2	103
149	Cortical dysplasia with prominent Rosenthal fiber formation in a case of intractable pediatric epilepsy. Human Pathology, 2009, 40, 1200-1204.	1.1	6
150	Activity in the fusiform face area supports expert perception in radiologists and does not depend upon holistic processing of images. Proceedings of SPIE, 2009, , .	0.8	5
151	Time course of imaging changes of GBM during extended bevacizumab treatment. Journal of Neuro-Oncology, 2008, 88, 339-347.	1.4	101
152	Phase II Pilot Study of Bevacizumab in Combination with Temozolomide and Regional Radiation Therapy for Up-Front Treatment of Patients With Newly Diagnosed Glioblastoma Multiforme: Interim Analysis of Safety and Tolerability. International Journal of Radiation Oncology Biology Physics, 2008, 71, 1372-1380.	0.4	169
153	A methodology to integrate clinical data for the efficient assessment of brain-tumor patients. Informatics for Health and Social Care, 2008, 33, 55-68.	1.4	4
154	Safety of anticoagulation use and bevacizumab in patients with glioma. Neuro-Oncology, 2008, 10, 355-360.	0.6	85
155	Relationship between Gene Expression and Enhancement in Glioblastoma Multiforme: Exploratory DNA Microarray Analysis. Radiology, 2008, 249, 268-277.	3.6	146
156	3-T Contrast-Enhanced MR Angiography in Evaluation of Suspected Intracranial Aneurysm: Comparison with MDCT Angiography. American Journal of Roentgenology, 2008, 190, 389-395.	1.0	32
157	Relationship between Survival and Edema in Malignant Gliomas: Role of Vascular Endothelial Growth Factor and Neuronal Pentraxin 2. Clinical Cancer Research, 2007, 13, 2592-2598.	3.2	108
158	Predicting Treatment Response of Malignant Gliomas to Bevacizumab and Irinotecan by Imaging Proliferation With [¹⁸ F] Fluorothymidine Positron Emission Tomography: A Pilot Study. Journal of Clinical Oncology, 2007, 25, 4714-4721.	0.8	400
159	Supraaortic Arteries: Contrast-enhanced MR Angiography at 3.0 T—Highly Accelerated Parallel Acquisition for Improved Spatial Resolution over an Extended Field of View. Radiology, 2007, 242, 600-609.	3.6	52
160	High Spatial-Resolution CE-MRA of the Carotid Circulation With Parallel Imaging. Investigative Radiology, 2006, 41, 391-399.	3.5	49
161	Contrast-enhanced MR angiography at 3T in the evaluation of intracranial aneurysms: a comparison with time-of-flight MR angiography. American Journal of Neuroradiology, 2006, 27, 2118-21.	1.2	44
162	18F-FDOPA PET imaging of brain tumors: comparison study with 18F-FDG PET and evaluation of diagnostic accuracy. Journal of Nuclear Medicine, 2006, 47, 904-11.	2.8	293

#	Article	IF	CITATIONS
163	<title>Integration of HIS/RIS clinical document with PACS image studies for neuroradiology</title> . , 2005, , .		4
164	MR imaging correlates of survival in patients with high-grade gliomas. American Journal of Neuroradiology, 2005, 26, 2466-74.	1.2	315
165	Microtubule-Associated Protein Tau Is Hyperphosphorylated during Mitosis in the Human Neuroblastoma Cell Line SH-SY5Y. Experimental Neurology, 1994, 126, 185-194.	2.0	97
166	Phosphorylated Tau Epitope of Alzheimer's Disease Is Coupled to Axon Development in the Avian Central Nervous System. Experimental Neurology, 1993, 120, 106-113.	2.0	45
167	Transient expression of adheron molecules during chick retinal development. Journal of Neurobiology, 1992, 23, 720-738.	3.7	3